OSR1 regulates a subset of inward rectifier potassium channels via a binding motif variant

Clinton A. Taylor IV[a], Sung-Wan An[b,1], Sachith Gallolu Kankanamalage[a], Steve Stippec[a], Svetlana Earnest[a], Ashesh T. Trivedi[a], Jonathan Zijiang Yang[a], Hamid Mirzaei[c], Chou-Long Huang[b,1,2], and Melanie H. Cobb[a,2]

[a]Department of Pharmacology, University of Texas Southwestern Medical Center, Dallas, TX 75390; [b]Department of Internal Medicine, University of Texas Southwestern Medical Center, Dallas, TX 75390; and [c]Department of Biochemistry, University of Texas Southwestern Medical Center, Dallas, TX 75390

Contributed by Melanie H. Cobb, March 2, 2018 (sent for review February 7, 2018; reviewed by Barbara E. Ehrlich, Shmuel Muallem, and Wen-Hui Wang)

The with-no-lysine (K) (WNK) signaling pathway to STE20/SPS1-related proline- and alanine-rich kinase (SPAK) and oxidative stress-responsive 1 (OSR1) kinase is an important mediator of cell volume and ion transport. SPAK and OSR1 associate with upstream kinases WNK 1–4, substrates, and other proteins through their C-terminal domains which interact with linear R-F-x-V/I sequence motifs. In this study we find that SPAK and OSR1 also interact with similar affinity with a motif variant, R-x-F-x-V/I. Eight of 16 human inward rectifier K^+ channels have an R-x-F-x-V motif. We demonstrate that two of these channels, Kir2.1 and Kir2.3, are activated by OSR1, while Kir4.1, which does not contain the motif, is not sensitive to changes in OSR1 or WNK activity. Mutation of the motif prevents activation of Kir2.3 by OSR1. Both siRNA knockdown of OSR1 and chemical inhibition of WNK activity disrupt NaCl-induced plasma membrane localization of Kir2.3. Our results suggest a mechanism by which WNK-OSR1 enhance Kir2.1 and Kir2.3 channel activity by increasing their plasma membrane localization. Regulation of members of the inward rectifier K^+ channel family adds functional and mechanistic insight into the physiological impact of the WNK pathway.

WNK1 | hypertension | SPAK | kinase cascade

The signaling pathway composed of the with-no-lysine (K) (WNK) protein kinases and their substrate protein kinases STE20/SPS1-related proline- and alanine-rich kinase (SPAK) and oxidative stress-responsive 1 (OSR1) is an important mediator of cell volume and ion transport that helps regulate blood pressure, neurotransmission, angiogenesis, and other physiological processes (1–4). The pathway has been linked to numerous disease states, including hypertension, neuropathies, and cancer (5–11).

Each of the four WNKs is activated by autophosphorylation in response to both low intracellular Cl^- and hyperosmotic stress (2, 12–14). WNKs then phosphorylate SPAK and OSR1, closely related Ste20 family kinases, at sites within their activation loops and C terminal to the end of the core kinase domain to increase their activities (Fig. 1*A*). The best-characterized regulation of ion transport by SPAK and OSR1 is through phosphorylation of the cytoplasmic regions of the SLC12 family of cation chloride cotransporters (NCC, NKCCs 1 and 2, and KCCs 1–4) (15). Phosphorylation of the cotransporters activates NCC and NKCCs and deactivates KCCs (16).

In addition to direct cotransporter phosphorylation by SPAK/OSR1, WNKs have also been shown to modulate activities of some ion channels and cotransporters proteins by altering their cell surface expression. WNK1 activation of SGK1 leads to the phosphorylation of E3 ubiquitin ligase Nedd4-2 which decreases its interaction with the epithelial Na^+ channel (ENaC) increasing its plasma membrane residence (17, 18). Mice overexpressing kidney-specific WNK1 (KS-WNK1) have decreased cell surface expression of NCC and NKCC2 in the distal convoluted tubule and thick ascending limb of the kidney, respectively (19, 20). KS-WNK1 lacks most of the kinase domain and antagonizes the effects of full-length WNK1 (21, 22). WNK1 and WNK4 inhibit ROMK (renal outer medullary potassium channel, Kir1.1), a member of the inward rectifier K^+ channel (IRK) family, by decreasing its cell surface expression (22). This occurs through interactions of either WNK1 or WNK4 with intersectin and ROMK in a kinase activity-independent manner (23). Regulation of ENaC and ROMK by WNKs, in addition to well-known effects of WNKs on cation chloride cotransporters NCC and NKCC2, likely contribute to hypertension and hyperkalemia in pseudohypoaldosteronism type II (PHA2), a single gene form of hypertension caused by increased expression of WNK1 or WNK4 (24–27).

Activation of SPAK and OSR1 by WNKs and regulation of SLC12 cotransporters depends on an interaction between the SPAK/OSR1 conserved C-terminal (CCT) domains, also called PF2 domains (P from PASK, another name for SPAK, and F from Fray, the *Caenorhabditis elegans* homolog), and linear sequence motifs in partners including WNKs and SLC12 cotransporters (28–31). This motif contains a consensus sequence of R-F-x-V/I. It has been generally accepted that this motif signature is strictly required for CCT interaction since its identification more than 15 years ago (28).

By examining the effects of mutations in known R-F-x-V/I motifs on CCT domain interactions we determined that the sequence

Significance

With-no-lysine (K) (WNK) protein kinases regulate ion transport. Mutations in WNKs 1 and 4 can cause a monogenic hypertension, pseudohypoaldosteronism type II (PHA2). The WNK-regulated protein kinases STE20/SPS1-related proline- and alanine-rich kinase (SPAK) and oxidative stress-responsive 1 (OSR1) mediate actions of WNKs on cation chloride cotransporters. The conserved C-terminal domains (CCTs) of OSR1/SPAK recognize linear R-F-x-V/I motifs in transporters and other protein targets. We discovered that OSR1/SPAK CCTs also recognize a motif variant, R-x-F-x-V/I, found in 8 of 16 inward rectifier K^+ (IRK) channels. We show that WNK and OSR1 regulate IRK channels, dependent on the presence of the variant motif. WNK kinase activity-dependent regulation of ion channels reveals a previously unknown mechanism and expands knowledge of potential WNK-OSR1/SPAK actions in cardiac and renal physiology.

Author contributions: C.A.T., S.-W.A., S.G.K., C.-L.H., and M.H.C. designed research; C.A.T., S.-W.A., S.G.K., S.S., S.E., A.T.T., J.Z.Y., and H.M. performed research; C.A.T., S.-W.A., S.G.K., S.S., S.E., H.M., C.-L.H., and M.H.C. analyzed data; and C.A.T., C.-L.H., and M.H.C. wrote the paper.

Reviewers: B.E.E., Yale University; S.M., National Institute of Health; and W.-H.W., New York Medical College.

The authors declare no conflict of interest.

[1]Present address: Division of Nephrology, Department of Internal Medicine, University of Iowa Carver College of Medicine, Iowa City, IA 52242.

[2]To whom correspondence may be addressed. Email: chou-long-huang@uiowa.edu or melanie.cobb@utsouthwestern.edu.

This article contains supporting information online at www.pnas.org/lookup/suppl/doi:10.1073/pnas.1802339115/-/DCSupplemental.

Published online March 26, 2018.

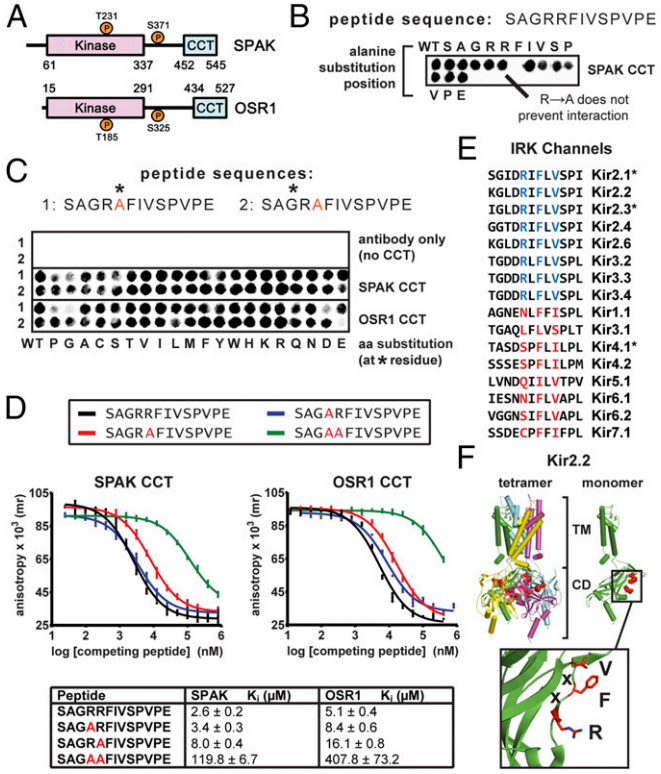

Peptide	SPAK K_i (μM)	OSR1 K_i (μM)
SAGRRFIVSPVPE	2.6 ± 0.2	5.1 ± 0.4
SAGARFIVSPVPE	3.4 ± 0.3	8.4 ± 0.6
SAGRAFIVSPVPE	8.0 ± 0.4	16.1 ± 0.8
SAGAAFIVSPVPE	119.8 ± 6.7	407.8 ± 73.2

Fig. 1. SPAK and OSR1 interact with the RFxV motif variant, RxFxV, and multiple members of the inward-rectifier K^+ (IRK) channel family contain the motif. (*A*) Domain organization of the closely related SPAK and OSR1 kinases. CCT domains are known to interact with RFxV motifs. (*B*) Membrane containing covalently linked peptides with the base sequence SAGRRFIVSPVPE where each residue of the sequence shown were mutated to alanine. Peptide interactions with His_6-SPAK CCT domain (residues 449–545) were determined by immunoblot with anti-His_6 antibody. (*C*) Immunoblot as in *B* examining interactions between His_6-SPAK CCT or His_6-OSR1 CCT domain (residues 433–527) and a peptide with the base sequence SAGRAFIVSPVPE. The asterisk (*) indicates the residue that was mutated in each sequence on the two rows. Letters at *Bottom* correspond to amino acid substitution. (*D*) Fluorescence polarization competitive binding assays. Fluorescent probe {NH_3^+-NLVGRF [DAP-FAM] VSPVPE-COO^-} [diaminopropionic acid (DAP)] held constant at 25 nM, SPAK CCT and OSR1 CCT held constant at 1.5 μM and 3.0 μM, respectively, and concentration of unlabeled peptides was varied. Red lettering indicates substitution to alanine on unlabeled peptides. (*E*) Multiple sequence alignment around the RxFxV motif found in IRK family members (blue lettering). Numbering for Kir2.1 is S256 to I267. Asterisk (*) indicates IRK channels investigated in this study. (*F*) Crystal structure of the Kir2.2 channel from *Gallus gallus* (PDB ID: 3JYC). The RxFxV motif (red) resides on a surface-exposed loop on the cytoplasmic domain (CD). TM, transmembrane.

R-x-F-x-V/I is also able to interact with similar affinity with CCT domains of OSR1 and SPAK. Eight of the 16 IRK channel family members [not including Kir1.1 (ROMK)] contain an R-x-F-x-V motif. IRK channels control essential processes throughout the body, including the circulatory system and vasculature as well as neuronal excitability (32–34). We tested 2 of the 8 IRK channels with the variant motif, Kir2.1 and Kir2.3, and found that their activities are regulated by OSR1. We confirmed that the motif is required for regulation of Kir2.3. Inhibition of WNKs or depletion of OSR1 also decreased the NaCl-induced plasma membrane localization of Kir2.3, suggesting a mechanism whereby WNK and SPAK/OSR1 regulate the activity of Kir2.3 by modulating the abundance of the channel at the cell surface. We suggest that other members of the IRK family may be regulated in a similar manner, extending the physiological impact of the WNK pathway.

Results

Evaluating R-F-x-V/I Binding Specificity on Peptide Arrays. SLC12 cation chloride cotransporters were originally found to be regulated by dephosphorylation by phosphoprotein phosphatase 1 (35), implying that a kinase was also required. This led to the identification of OSR1 and SPAK as the cotransporter regulatory kinases (28, 36). At the same time SPAK/OSR1 were shown to bind directly to multiple SLC12 cotransporters through their conserved CCT domains. From examining the interacting regions, a nine residue sequence was implicated in binding the CCT with highly conserved residues yielding the R-F-x-V/I motif (28). The binding mode and importance of the conserved residues of the motif was subsequently revealed through determination of the CCT domain structure (37). Several motifs are present in WNK1 that bind SPAK and OSR1 (3, 31, 38). To evaluate relative interactions with different R-F-x-V/I motifs, we tested binding of purified OSR1 and SPAK CCT domains (Fig. 1*A*) to membranes spotted with systematically mutated synthetic peptides derived from the motif to generate a higher volume peptide binding assay (Fig. 1*B*).

R-x-F-x-V/I Is an Alternative SPAK/OSR1 CCT Domain Binding Motif. To determine the contribution of each residue within the human WNK1-derived peptide, ^{1253}SAGRRFIVSPVPE^{1265} (accession Q9H4A3) to human His_6-tagged SPAK CCT domain (residues 449–545), we incubated His_6-SPAK CCT with a membrane containing an immobilized peptide array with each position along the peptide mutated to alanine and identified CCT binding by immunoblotting with an anti-His_6 antibody (Fig. 1*B*). As expected, mutation of F1258 and V1260 led to significant disruption of the interaction, as did mutation of the residues S1261 and P1262, which follow the motif. An unanticipated result was that mutation of R1257 to alanine did not significantly disrupt binding, implying that an arginine, one position displaced (R1256), was capable of substituting for the arginine known to be required for a functional motif (R1257).

To further investigate whether R-x-F-x-V/I is an alternative SPAK/OSR1 CCT interaction motif, we used the same peptide but with the substitution R1257A and systematically mutated the positions on either side of R1256 to every other amino acid to determine the effects on binding His_6-SPAK CCT and His_6-OSR1 CCT (residues 433–527). Using the same immobilized peptide immunoblot methodology in peptide array format (Fig. 1*C*), we found that R1257 could be mutated (to any amino acid except P, G, or D) without significant loss of binding, and G1255 could be mutated to any amino acid except E. A proline in place of arginine at position 1257 will diminish peptide backbone flexibility, while a glycine will enhance flexibility; introducing negative charges at positions 1255 and 1257 (G1255D or R1257E) are likely to diminish the electrostatic interaction with the negatively charged peptide binding surface of the CCT domain. These results suggest that the alternative position of the arginine in R-x-F-x-V/I is not dependent on the amino acid identity of the flanking residues because nearly all of the substituted peptides still bound the CTT domain.

We then measured fluorescence anisotropy in peptide binding competition assays to quantify the binding (K_i) of wild-type and mutant WNK1 peptides to the His_6-OSR1 CCT and His_6-SPAK CCT domains (Fig. 1*D*). We developed a fluorescent peptide probe, NH_3^+-NLVGRF[DAP-FAM] VSPVPE-COO^- [diaminopropionic acid (DAP)] that is a chimera of WNK4 and WNK1 R-F-x-V peptide sequences with an internally incorporated fluorescein derivative (FAM) conjugated to diaminopropionic acid. This probe has affinities (K_d) of 0.70 ± 0.10 μM for His_6-SPAK CCT and 1.6 ± 0.3 μM for His_6-OSR1 CCT (*SI Appendix*, Fig. S1*A*).

Affinities for the unlabeled WNK1 peptides to the His_6-OSR1 CCT were 5.1 ± 0.4 μM for wild type, 8.4 ± 0.6 μM for R1256A, 16.1 ± 0.8 μM for R1257A, and 410 ± 72 μM for R1256A/R1257A, while affinities for the peptides to the His_6-SPAK CCT were 2.6 ± 0.2 μM for wild type, 3.4 ± 0.3 μM for R1256A, 8.0 ± 0.4 μM for R1257A, and 120 ± 7 μM for R1256A/R1257A

(Fig. 1*D*). The binding constants were weaker by ~40- to 50-fold for peptides lacking both arginines, but within 2- to 3-fold of the wild-type peptide if one or the other arginine was mutated. These results indicate that it is possible for motifs containing arginine at either position to bind SPAK or OSR1 CCT domains with similar affinities in the case of the WNK1 1253–1265 peptide. The quantitative anisotropic data and semiquantitative peptide array data show that R-x-F-x-V/I is also a valid SPAK/OSR1 CCT domain binding motif (Fig. 1 *C* and *D*).

OSR1 Kinase Activity Enhances Kir2.1 and Kir2.3 Channel Activity. We examined proteins that contained R-x-F-x-V/I motifs and found that 8 of 16 IRK channel family members contain the sequence R-x-F-x-V (Fig. 1*E*). All of the Kir2.x and some of the Kir3.x IRK family members contain the motif, while ROMK (Kir1.1), which is known to be regulated by WNK kinases via a kinase activity-independent mechanism, does not. The motifs from the 8 IRK family members are conserved in both mouse and frog, are predicted to be present in the cytosol, and lie on solvent-accessible loops exposed in the monomeric forms of IRK channels based on the crystal structure of Kir2.2 and other IRK channels (39, 40) (Fig. 1*F*). The functional channel is a tetramer, and the motif-containing loop is partially buried in the interface between cytoplasmic domains (CDs) of the subunits in the IRK channel tetramer. A peptide corresponding to the Kir2.3 motif, RIFLVSP, bound to the OSR1 CCT domain (*SI Appendix*, Fig. S1*B*).

We investigated the influence of kinase activity on IRK channel activity in cells. We compared effects of wild-type OSR1 and an active OSR1 mutant in which the two WNK phosphorylation sites, T185, within the activation loop, and S325, immediately following the core kinase domain, were mutated to glutamate (Fig. 1*A*). Coexpression of active OSR1 T185E/S325E ($OSR1^{CA}$) and Kir2.1 in HEK293 cells led to nearly a 2.5-fold increase in Kir2.1 channel activity, measured as current density by whole-cell patch clamp, compared with Kir2.1 alone (Fig. 2 *A* and *C*). Coexpression of $OSR1^{CA}$ and Kir4.1, which does not have an R-x-F-x-V motif, did not result in an increase in activity compared with channel alone (Fig. 2 *B* and *C*). Current density was roughly proportional to the amount of DNA transfected and in neither case did OSR1 affect current from Kir4.1. Kir2.1 coexpressed with wild-type OSR1 had activity similar to the vector control, as did coexpression of the the channel with the OSR1-activating kinase, WNK1 alone (Fig. 2*D*). However, coexpression with both WNK1 and wild-type OSR1 led to an increase in Kir2.1 channel activity, which approached that caused by $OSR1^{CA}$. These results demonstrate that active OSR1 increases Kir2.1 channel activity (Fig. 2).

To further substantiate the ability of the variant motif to confer regulation by WNK1/OSR1, we tested a second channel, Kir2.3. Expression of Kir2.3 with wild-type OSR1 led to an increase in Kir2.3 channel activity, that was further increased by coexpressing the channel with the active mutant $OSR1^{CA}$. A twofold increase in channel activity was observed (Fig. 3*A*). Coexpression of Kir2.3 with $OSR1^{CA}$ lacking its CCT domain ($OSR1^{CA\Delta CCT}$) or mutated to impair kinase activity ($OSR1^{CA/KD}$, D146N) resulted in no change in channel activity, suggesting that both the ability of OSR1 to bind the motif through its CCT and OSR1 catalytic activity were required for the increase in channel activity. The finding that channel activity was above that in cells expressing vector control may be due to the ability of OSR1 to form active dimers with endogenous protein (41).

To determine whether the increase in activity of Kir2.3 in the presence of wild-type OSR1 was aided by endogenous WNK1, we performed similar experiments but in cells in which WNK1 was depleted using siRNA (Fig. 3*B*). Reduced WNK1 expression did not change channel activity in cells expressing the vector control or active $OSR1^{CA}$, but resulted in Kir2.3 activity in cells expressing wild-type OSR1 that was similar to that in cells expressing the vector control. These findings suggest that endogenous WNK1 increases the activity of OSR1 which causes the increase in Kir2.3 channel activity.

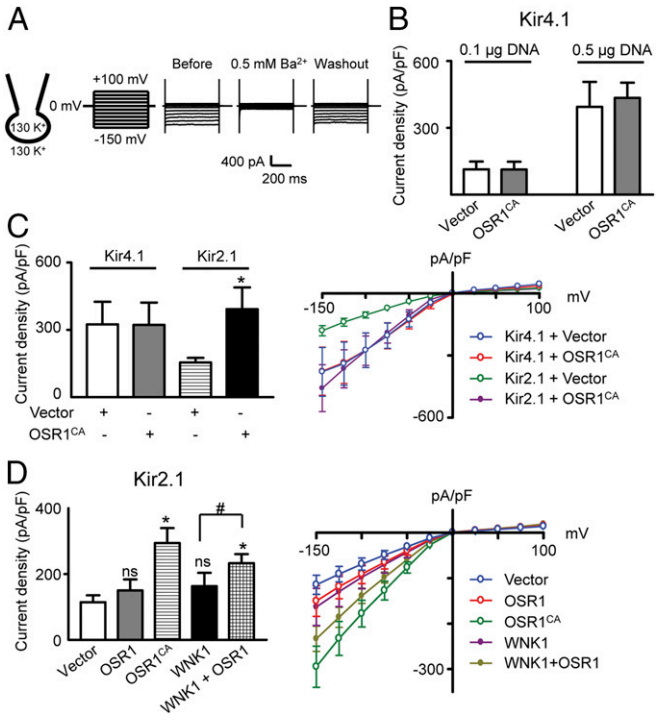

Fig. 2. Constitutively active OSR1 ($OSR1^{CA}$; T185E/S325E) enhances Kir2.1 but not Kir4.1 channel activity. (*A*) Whole-cell patch clamp experimental parameters used in study. In all experiments HEK293 cells were cotransfected with both an IRK channel and an additional overexpression vector as indicated. (*B*) Inward current density (pA at −150 mV/pF) measured in cells overexpressing both Kir4.1 and either vector control or $OSR1^{CA}$. Measurements were done using either 0.1 or 0.5 µg Kir4.1 expression vector. (*C*) Comparison of current density of Kir2.1 and Kir4.1 in the presence or absence of $OSR1^{CA}$. $^{*}P \leq 0.05$, $OSR1^{CA}$ vs. vector. (*D*) Current density of Kir2.1 in the presence or absence of various WNK pathway components. WNK1 + OSR1 measurement involved cotransfection of three separate vectors. ns, not significant; $^{*}P \leq 0.05$ vs. vector (first bar from *Left*); $^{\#}P < 0.05$ between indicated bars.

To assess whether the Kir2.3 R-x-F-x-V motif was required for sensitivity to regulation by OSR1, we mutated the motif in Kir2.3 by removing the essential R252 and replacing it with lysine or alanine. Kir2.3 R252K expressed with vector control displayed only a minor decrease in channel activity compared with wild type (Fig. 3*C*). The mutation did not significantly impact oligomerization of the cytoplasmic domain, as assessed by gel filtration (Fig. 3*D*). Kir2.3 R252A had much reduced channel activity, most likely because a positive charge at that position in the interface is required for formation of the functional tetramer. The Kir2.3 channel mutants were coexpressed with $OSR1^{CA}$ (Fig. 3*C*). Neither Kir2.3 R252K nor R252A exhibited an increase in activity in the presence of $OSR1^{CA}$. These findings provide additional evidence that the motif confers sensitivity to regulation of channel activity by OSR1.

NaCl-Induced Kir2.3 Plasma Membrane Localization Is Reduced by Inhibition of WNK Signaling. OSR1 and SPAK phosphorylate cation chloride cotransporters to regulate their activity. To determine whether OSR1 or SPAK phosphorylate Kir2.3, we assessed SPAK and OSR1 kinase activity toward the cytoplasmic region of Kir2.3 (Δ55–172-$Kir2.3_{cyto}$) tagged with maltose binding protein that had been expressed in bacteria (MBP-$Kir2.3_{cyto}$) (40). SPAK 62–556 T243E, encompassing the kinase and CCT domains, and OSR1 T185D showed no appreciable activity toward MBP-$Kir2.3_{cyto}$ (*SI Appendix*, Fig. S2). Under the

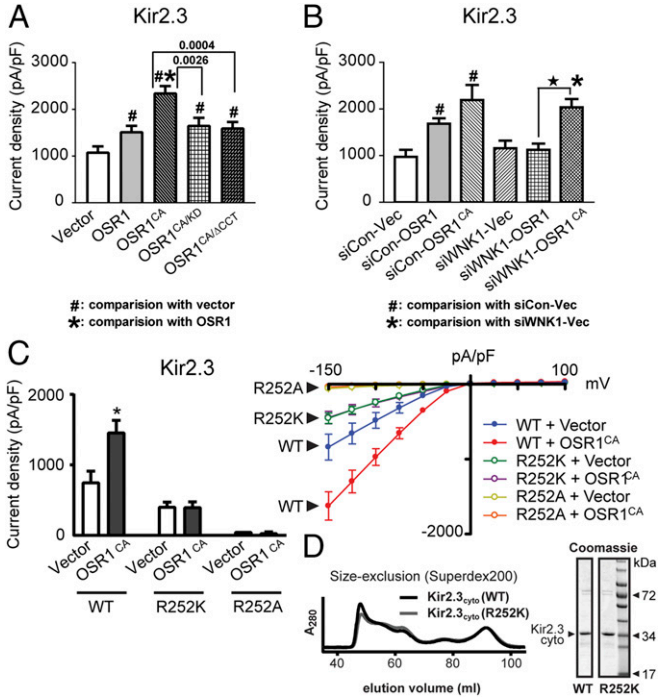

Fig. 3. OSR1^{CA} enhances Kir2.3 channel activity and RxFxV motif integrity is required. (*A*) Current density in HEK293 cells coexpressing Kir2.3 and either vector control or wild-type or mutant versions of OSR1. OSR1$^{CA/KD}$ is OSR1 T185E/S325E/D146N (constitutively active, kinase dead). OSR1$^{CA/\Delta CCT}$ is OSR1 T185E/S325E/ΔA434-527 (lacking CCT domain). (*B*) Current density in cells coexpressing Kir2.3 and either vector control, OSR1, or OSR1^{CA} in the presence of either siRNA control or siRNA targeting WNK1 (siWNK1). *$P \leq 0.05$. (*C*) Current density in cells coexpressing wild-type or mutant forms of Kir2.3 and either vector control or OSR1^{CA}. R252 is the arginine in the RxFxV motif. *$P \leq 0.05$. Current density lines for R252A mutant plus vector (yellow) and OSR^{CA} (orange) overlap with the *x* axis. Lines for R252K (green and purple) overlap with each other. (*D*) Size-exclusion chromatography on Superdex200 resin of His$_6$-tagged Kir2.3$_{cyto}$ WT or R252K (N-terminal His$_6$-tagged internal Kir2.3 fusion consisting of the channel cytoplasmic region with the transmembrane and extracellular loop residues 55–172 deleted). Void volume is ∼45 mL. Coomassie-stained gel of samples used for the experiment are presented.

same conditions, GST-NKCC2 1–175, a well characterized SPAK/OSR1 substrate, was highly phosphorylated as deduced by phosphate incorporation and gel shift. The addition of Mo25α, which further activates SPAK and OSR1 by nearly 100-fold, did not induce phosphorylation (42, 43). Analysis of Kir2.3 by mass spectrometry from in vitro labeling and from intact cells, did not reveal posttranslational modifications that were associated with the presence of OSR1^{CA} or SPAK 62–556 T243E (data not shown). Under the conditions tested, there is no clearly defined phosphorylation of Kir2.3, suggesting that SPAK and OSR1 do not regulate Kir2.3 channel activity by phosphorylating the channels themselves.

Several channels and cotransporters are regulated by WNKs by a change in protein localization (23, 44–47). Therefore, we examined the effects of manipulating WNK and OSR1 activity on the localization of Kir2.3. To detect the channel, a FLAG tag was inserted between residues A95 and A96 in the extracellular loop. In cells in standard medium, Kir2.3 appeared most concentrated in the perinuclear region with some diffuse in the cytoplasm. Because NaCl activates WNKs and OSR1/SPAK, we assessed effects of NaCl on the channel. Addition of 150 mM NaCl to the medium increased the percentage of cells with Kir2.3 near the plasma membrane (Fig. 4*A*). Increased localization at the cell surface could account for the increase in Kir2.3 activity. To determine whether OSR1 was important for the changes in localization, we knocked down OSR1 using siRNA, and found that depleted OSR1 prevented NaCl-induced membrane localization of Kir2.3 and appeared to reduce its cytoplasmic distribution as well (Fig. 4*A*). OSR1 knockdown did not affect the amount of Kir2.3 expressed (*SI Appendix*, Fig. S3). Similarly, treatment with the pan-WNK inhibitor, WNK463, also significantly decreased the NaCl-induced membrane localization of Kir2.3 (Fig. 4*B*). We interpret these results to indicate that activation of WNK pathway signaling leads to an increase in Kir2.3 at the cell surface, thereby increasing current density (*SI Appendix*, Fig. S5).

Discussion

The Ste20 family kinases SPAK and OSR1 contain a ∼90 residue CCT domain that binds short linear R-F-x-V/I motifs that were identified more than 15 years ago (28). In analyzing CCT domain specificity for residues in a WNK1 motif, we found that the CCT domain can also accommodate the insertion of a residue between the arginine and phenylalanine in the linear motif. A simple molecular model of the OSR1 CCT bound to a AAR-AFQVT peptide based on the structure of OSR1 CCT bound to a GRFQVT peptide further supports this idea (*SI Appendix*, Fig. S4). Binding is maintained with residues adjacent and on either side of the arginine mutated to most other amino acids. In examining the structure of the CCT domain, the RxFxV motif can assume a conformation that allows it to fit into the pocket. The positions of the C_β carbons on the residues adjacent to the arginine in the model support this idea (*SI Appendix*, Fig. S4). Interestingly, all four of the KCCs in the SLC12 family have a variant motif that may enable them to interact with OSR1 and SPAK. WNKs regulate the activity of KCCs, but only two of the KCCs have the typical R-F-x-V motif. Only one interaction between an R-F-x-V fragment of KCC3 and the SPAK and OSR1 CCTs has been demonstrated by yeast two hybrid screening (28).

The plasma membrane localization of Kir2.3 was increased by NaCl in the presence of OSR1. What is not yet clear from our analysis is why the kinase activity of OSR1 is needed to increase channel activity when the channel itself is not a substrate. In vitro, active SPAK/OSR1 did not phosphorylate the intracellular domain of the channel even under conditions in which all of an intracellular fragment of NKCC2, a known substrate, displayed an altered electrophoretic mobility after phosphorylation. The CCT is connected to the kinase domain by nearly 100 residues with little predicted structure. The likely flexibility of this CCT linker may provide the kinase domain access to substrates more than 100 Å from the CCT-bound channel. Because the translocation of the channel is dependent on OSR1, regulation of trafficking mechanisms by phosphorylation must be considered likely possibilities. Intersectin binds to WNKs and mediates WNK-dependent endocytosis of ROMK. Although WNK kinase activity is not required, intersectin is highly phosphorylated and may be subject to functional regulation by OSR1/SPAK under certain circumstances. Sortilin, which also contains an R-F-x-V motif, has been implicated in WNK4-dependent trafficking of NCC to lysosomes in Cos-7 cells, for example. NCC colocalized with a lysosomal marker in a perinuclear pattern, reminiscent of Kir2.3 staining with OSR1 depletion (20). Few of the numerous phosphorylation sites in intersectin and sortilin are understood functionally. Several E3 ubiquitin ligases such as Nedd4-2 and Kelch-like proteins with cullin E3 ligases may also participate in controlling the kinase activity-dependent localization of Kir2.3 (18, 26, 27, 48).

Proteins that rely on binding to the Kir2.x C-terminal PDZ domain binding motif are known to form multiprotein complexes with Kir2.x and these may be linked to OSR1/SPAK regulation of the channels (49). For example, Tax-interacting protein-1 (TIP-1) is known to enhance internalization of Kir2.3 through PDZ domain interaction with the C terminus of Kir2.3. Phosphorylation of the C-terminal Kir2.3 PDZ binding motif, presumably by PKA, prevents TIP-1–mediated internalization (50). Kir2.3 has also been shown to be constitutively internalized via an AP-2 clathrin-dependent mechanism

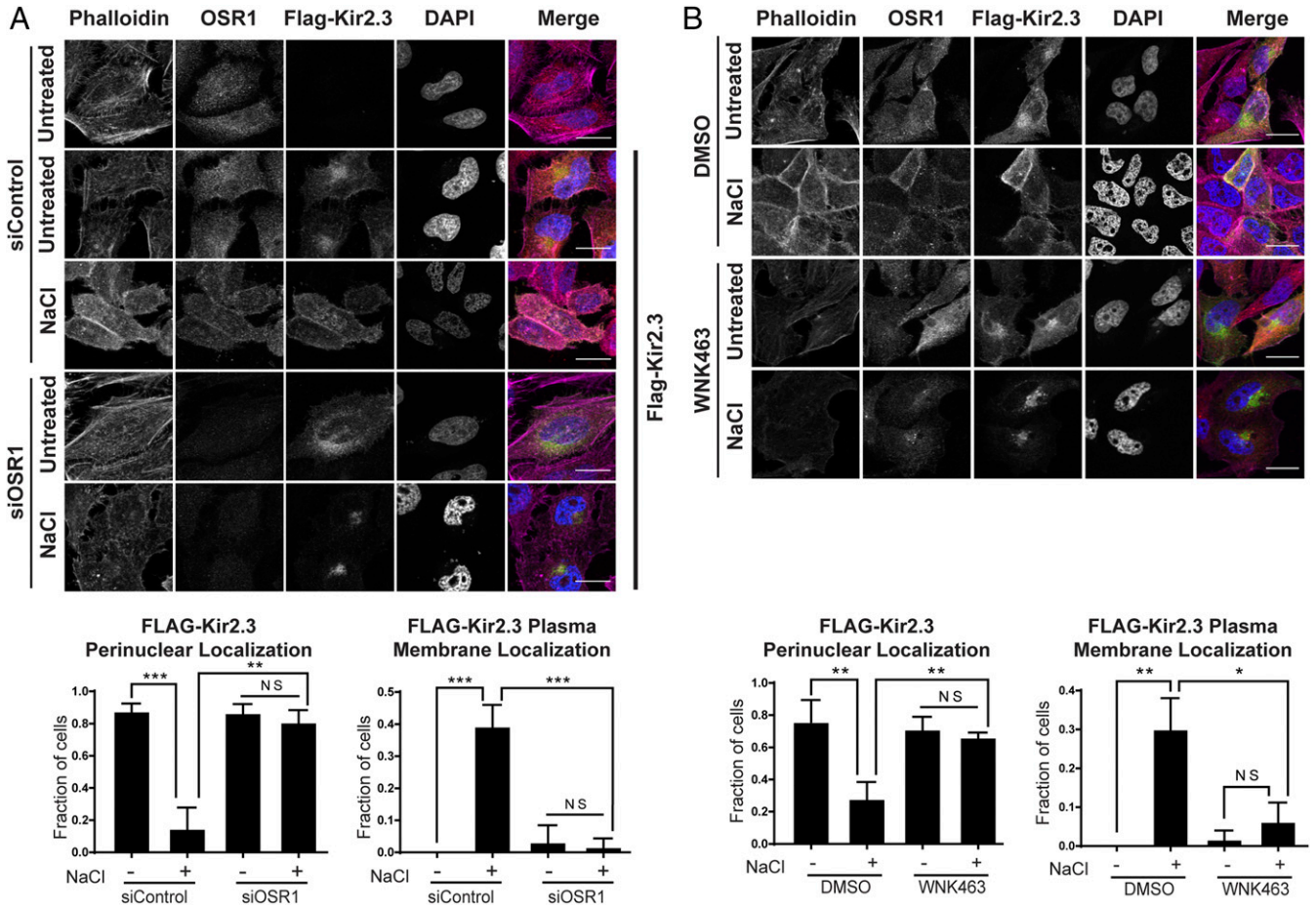

Fig. 4. siRNA knockdown of OSR1 and chemical inhibition of WNK kinases disrupt NaCl induced plasma membrane localization of Kir2.3. (*A*) HeLa cells overexpressing Flag-Kir2.3 (3xFlag between A95 and A96 in extracellular loop), except for first row, were treated with ±150 mM NaCl and ±OSR1 siRNA (siOSR1). Fluorescence microscopy images were obtained for staining with indicated antibodies or chemicals (*Top* labels). Cells were categorized independently both based on whether they had a primarily perinuclear and plasma membrane localization. NS, not significant, $^{**}P \leq 0.01$, $^{***}P \leq 0.001$. (*B*) As in *A* except ±WNK inhibitor WNK463 instead of ±siOSR1. NS, not significant, $^{*}P \leq 0.05$, $^{**}P \leq 0.01$.

(51). OSR1/SPAK might reduce either TIP-1 or AP-2 clathrin-dependent Kir2.3 internalization.

Transcellular Na^+ reabsorption by the distal nephron of the kidney involves Na^+ entry from the urinary space into cells through the apical epithelial Na^+ channel ENaC. WNK1 stimulates ENaC and inhibits the K^+ channel ROMK in the apical membrane of the connecting tubule and the cortical collecting duct. Both of these channels are controlled by kinase activity-independent mechanisms (18, 23). Na^+ that enters the cells from the urine is moved across the basolateral membrane into the circulation by Na^+-K^+-ATPase which results in K^+ accumulation in cells. The exit of K^+ from the cells is essential for continued Na^+ extrusion by Na^+-K^+-ATPase. Kir2.3 is present in the basolateral membrane of the distal nephron (52) and may fill this required function by mediating K^+ exit from the cells across the basolateral membrane into the circulation. Stimulation of Kir2.3 by WNK1-OSR1 would therefore be expected to increase transcellular Na^+ reabsorption by the distal nephron, which may contribute to hypertension in patients with PHA2 caused by gain-of-function WNK1 mutations.

Kir2.1, Kir2.2, and Kir2.3 have established functions in heart, brain, skeletal muscle, and the vasculature, as well as less defined roles in other tissues (32). In cardiomyocytes, the current carried by IRK channels is central to determining the characteristics of the cardiac action potential (34). Kir2.x channel subunits are crucial for maintaining the resting membrane potential and excitability of certain neurons, and Kir 2.1 is involved in regulating blood pressure (33). These physiological processes may also be modulated by actions of the WNK-OSR1/SPAK pathway on these and additional IRK channels with the variant CCT binding motif.

Methods

Additional methods appear in *SI Appendix, Extended Methods*.

Membrane-Immobilized Peptide Blots. Immobilized peptide membranes were purchased from Kinexus Bioinformatics Corp. Approximately 200 nmol of N-terminal acetylated peptides per spot was chemically synthesized on a TOTD membrane by coupling of the C terminus of the peptide to the membrane, and peptide synthesis was carried out on the membrane. Membranes were rinsed with EtOH, then washed for 30 min with TBST (0.1% Tween). Membranes were blocked for 60 min with 1:1 Odyssey blocking buffer to TBST [blocking solution, incubated with 300 μM His_6-SPAK CCT (residues 449–545) or His_6-OSR1 CCT (residues 433–527)] in blocking solution for 60 min, washed 2 × 5 min in TBST, incubated with 1:1,000 mouse anti-His_6 antibody (Clontech) for 15 min, and washed 2 × 5 min in TBST followed by incubation with 1:500 LI-COR IRDye 680RD mouse secondary antibody for 15 min. Membranes were washed 4 × 5 min in TBST before quantification by LI-COR Odyssey.

Fluorescence Polarization. His_6-SPAK CCT at 1.5 μM or 3.0 μM His_6-OSR1 CCT was combined with 25 nM NH_3^+-NLVGRF[DAP-FAM]VSPVPE-COO^- in 25 mM Tris·HCl pH 7.75 (at 25 °C), 125 mM NaCl, and 1 mM DTT and unlabeled competing peptides. Fluorescence polarization was measured (emission max, 485 nm; excitation max, 528 nm; 510 nm dichroic mirror).

Cell Culture and Transfection. HeLa cells expressed 3xFlag-Kir2.3 (A95-A96) as described in *SI Appendix, Extended Methods*.

Patch-Clamp Recordings. Patch-clamp recordings on HEK293 expressing Kir channels and WNK1/OSR1 were made as described in *SI Appendix, Extended Methods*.

Immunofluorescence, SDS/PAGE, and Immunoblotting. The methods for immunofluorescence, SDS/PAGE, and immunoblotting are similar to those described in ref. 53 and are presented in detail in *SI Appendix, Extended Methods*.

ACKNOWLEDGMENTS. We thank members of the M.H.C. laboratory and Kate Luby-Phelps [Department of Cell Biology and Live Cell Imaging Facility, University of Texas Southwestern (UT Southwestern)] for their suggestions about this project and Dionne Ware for administrative support. The work was supported by Welch Foundation Grant I1243 (to M.H.C.), National Institutes of Health Grants R37DK34128 (to M.H.C.) and R01DK111542 (to C.-L.H.), and National Cancer Institute Grant P30CA142543 to the Harold C. Simmons Comprehensive Cancer Center for partial support of the Live Cell Imaging Facility. A.T.T. was supported by the Summer Undergraduate Research Fellowship Program, and J.Z.Y. was supported by the STARS Student Summer Research Program, both at UT Southwestern.

1. Vitari AC, Deak M, Morrice NA, Alessi DR (2005) The WNK1 and WNK4 protein kinases that are mutated in Gordon's hypertension syndrome phosphorylate and activate SPAK and OSR1 protein kinases. *Biochem J* 391:17–24.
2. Moriguchi T, et al. (2005) WNK1 regulates phosphorylation of cation-chloride-coupled cotransporters via the STE20-related kinases, SPAK and OSR1. *J Biol Chem* 280: 42685–42693.
3. Anselmo AN, et al. (2006) WNK1 and OSR1 regulate the Na+, K+, 2Cl– cotransporter in HeLa cells. *Proc Natl Acad Sci USA* 103:10883–10888.
4. Xie J, et al. (2009) Endothelial-specific expression of WNK1 kinase is essential for angiogenesis and heart development in mice. *Am J Pathol* 175:1315–1327.
5. McCormick JA, Ellison DH (2011) The WNKs: Atypical protein kinases with pleiotropic actions. *Physiol Rev* 91:177–219.
6. Rafiqi FH, et al. (2010) Role of the WNK-activated SPAK kinase in regulating blood pressure. *EMBO Mol Med* 2:63–75.
7. Shekarabi M, et al. (2008) Mutations in the nervous system–Specific HSN2 exon of WNK1 cause hereditary sensory neuropathy type II. *J Clin Invest* 118:2496–2505.
8. Gagnon KB, Delpire E (2012) Molecular physiology of SPAK and OSR1: Two Ste20-related protein kinases regulating ion transport. *Physiol Rev* 92:1577–1617.
9. Gagnon KB, Delpire E (2013) Physiology of SLC12 transporters: Lessons from inherited human genetic mutations and genetically engineered mouse knockouts. *Am J Physiol Cell Physiol* 304:C693–C714.
10. Huang CL, Cheng CJ (2015) A unifying mechanism for WNK kinase regulation of sodium-chloride cotransporter. *Pflugers Arch* 467:2235–2241.
11. Yang L, et al. (2013) STE20/SPS1-related proline/alanine-rich kinase is involved in plasticity of GABA signaling function in a mouse model of acquired epilepsy. *PLoS One* 8:e74614.
12. Xu B, et al. (2000) WNK1, a novel mammalian serine/threonine protein kinase lacking the catalytic lysine in subdomain II. *J Biol Chem* 275:16795–16801.
13. Piala AT, et al. (2014) Chloride sensing by WNK1 involves inhibition of autophosphorylation. *Sci Signal* 7:ra41.
14. Wu Y, Schellinger JN, Huang CL, Rodan AR (2014) Hypotonicity stimulates potassium flux through the WNK-SPAK/OSR1 kinase cascade and the Ncc69 sodium-potassium-2-chloride cotransporter in the Drosophila renal tubule. *J Biol Chem* 289:26131–26142.
15. Darman RB, Forbush B (2002) A regulatory locus of phosphorylation in the N terminus of the Na-K-Cl cotransporter, NKCC1. *J Biol Chem* 277:37542–37550.
16. Alessi DR, et al. (2014) The WNK-SPAK/OSR1 pathway: Master regulator of cation-chloride cotransporters. *Sci Signal* 7:re3.
17. Debonneville C, et al. (2001) Phosphorylation of Nedd4-2 by Sgk1 regulates epithelial Na(+) channel cell surface expression. *EMBO J* 20:7052–7059.
18. Xu BE, et al. (2005) WNK1 activates SGK1 to regulate the epithelial sodium channel. *Proc Natl Acad Sci USA* 102:10315–10320.
19. Liu Z, et al. (2011) Downregulation of NCC and NKCC2 cotransporters by kidney-specific WNK1 revealed by gene disruption and transgenic mouse models. *Hum Mol Genet* 20:855–866.
20. Cai H, et al. (2006) WNK4 kinase regulates surface expression of the human sodium chloride cotransporter in mammalian cells. *Kidney Int* 69:2162–2170.
21. Lazrak A, Liu Z, Huang CL (2006) Antagonistic regulation of ROMK by long and kidney-specific WNK1 isoforms. *Proc Natl Acad Sci USA* 103:1615–1620.
22. Liu Z, Wang HR, Huang CL (2009) Regulation of ROMK channel and K+ homeostasis by kidney-specific WNK1 kinase. *J Biol Chem* 284:12198–12206.
23. He G, Wang HR, Huang SK, Huang CL (2007) Intersectin links WNK kinases to endocytosis of ROMK1. *J Clin Invest* 117:1078–1087.
24. Wilson FH, et al. (2001) Human hypertension caused by mutations in WNK kinases. *Science* 293:1107–1112.
25. Louis-Dit-Picard H, et al.; International Consortium for Blood Pressure (ICBP) (2012) KLHL3 mutations cause familial hyperkalemic hypertension by impairing ion transport in the distal nephron. *Nat Genet* 44:456–460, S1–S3, and erratum (2012) 44:609.
26. Ohta A, et al. (2013) The CUL3-KLHL3 E3 ligase complex mutated in Gordon's hypertension syndrome interacts with and ubiquitylates WNK isoforms: Disease-causing mutations in KLHL3 and WNK4 disrupt interaction. *Biochem J* 451:111–122.
27. Shibata S, Zhang J, Puthumana J, Stone KL, Lifton RP (2013) Kelch-like 3 and Cullin 3 regulate electrolyte homeostasis via ubiquitination and degradation of WNK4. *Proc Natl Acad Sci USA* 110:7838–7843.
28. Piechotta K, Lu J, Delpire E (2002) Cation chloride cotransporters interact with the stress-related kinases Ste20-related proline-alanine-rich kinase (SPAK) and oxidative stress response 1 (OSR1). *J Biol Chem* 277:50812–50819.
29. Delpire E, Gagnon KB (2007) Genome-wide analysis of SPAK/OSR1 binding motifs. *Physiol Genomics* 28:223–231.
30. Vitari AC, et al. (2006) Functional interactions of the SPAK/OSR1 kinases with their upstream activator WNK1 and downstream substrate NKCC1. *Biochem J* 397:223–231.
31. Sengupta S, et al. (2012) Interactions with WNK (with no lysine) family members regulate oxidative stress response 1 and ion co-transporter activity. *J Biol Chem* 287: 37868–37879.
32. Cheng CJ, Sung CC, Huang CL, Lin SH (2015) Inward-rectifying potassium channelopathies: New insights into disorders of sodium and potassium homeostasis. *Pediatr Nephrol* 30:373–383.
33. Ahn SJ, et al. (2017) Inwardly rectifying K^+ channels are major contributors to flow-induced vasodilatation in resistance arteries. *J Physiol* 595:2339–2364.
34. Hibino H, et al. (2010) Inwardly rectifying potassium channels: Their structure, function, and physiological roles. *Physiol Rev* 90:291–366.
35. Darman RB, Flemmer A, Forbush B (2001) Modulation of ion transport by direct targeting of protein phosphatase type 1 to the Na-K-Cl cotransporter. *J Biol Chem* 276:34359–34362.
36. Dowd BF, Forbush B (2003) PASK (proline-alanine-rich STE20-related kinase), a regulatory kinase of the Na-K-Cl cotransporter (NKCC1). *J Biol Chem* 278:27347–27353.
37. Villa F, et al. (2007) Structural insights into the recognition of substrates and activators by the OSR1 kinase. *EMBO Rep* 8:839–845.
38. Thastrup JO, et al. (2012) SPAK/OSR1 regulate NKCC1 and WNK activity: Analysis of WNK isoform interactions and activation by T-loop trans-autophosphorylation. *Biochem J* 441:325–337.
39. Tao X, Avalos JL, Chen J, MacKinnon R (2009) Crystal structure of the eukaryotic strong inward-rectifier K+ channel Kir2.2 at 3.1 A resolution. *Science* 326:1668–1674.
40. Pegan S, et al. (2005) Cytoplasmic domain structures of Kir2.1 and Kir3.1 show sites for modulating gating and rectification. *Nat Neurosci* 8:279–287.
41. Taylor CA, 4th, et al. (2015) Domain-swapping switch point in Ste20 protein kinase SPAK. *Biochemistry* 54:5063–5071.
42. Ponce-Coria J, Gagnon KB, Delpire E (2012) Calcium-binding protein 39 facilitates molecular interaction between Ste20p proline alanine-rich kinase and oxidative stress response 1 monomers. *Am J Physiol Cell Physiol* 303:C1198–C1205.
43. Grimm PR, et al. (2012) SPAK, OSR1 and Cab39/MO25 form an interdependent signaling system which regulates thiazide-sensitive salt transport, distal tubule mass and blood pressure. *FASEB J* 26(Suppl 1):867.37.
44. Yang SS, et al. (2005) Regulation of apical localization of the thiazide-sensitive NaCl cotransporter by WNK4 in polarized epithelial cells. *Biochem Biophys Res Commun* 330:410–414.
45. Cope G, et al. (2006) WNK1 affects surface expression of the ROMK potassium channel independent of WNK4. *J Am Soc Nephrol* 17:1867–1874.
46. Subramanya AR, Liu J, Ellison DH, Wade JB, Welling PA (2009) WNK4 diverts the thiazide-sensitive NaCl cotransporter to the lysosome and stimulates AP-3 interaction. *J Biol Chem* 284:18471–18480.
47. Zhou B, et al. (2010) WNK4 enhances the degradation of NCC through a sortilin-mediated lysosomal pathway. *J Am Soc Nephrol* 21:82–92.
48. Roy A, et al. (2015) Alternatively spliced proline-rich cassettes link WNK1 to aldosterone action. *J Clin Invest* 125:3433–3448.
49. Leonoudakis D, et al. (2004) Protein trafficking and anchoring complexes revealed by proteomic analysis of inward rectifier potassium channel (Kir2.x)-associated proteins. *J Biol Chem* 279:22331–22346.
50. Yan X, et al. (2009) Molecular mechanism of inward rectifier potassium channel 2.3 regulation by tax-interacting protein-1. *J Mol Biol* 392:967–976.
51. Mason AK, Jacobs BE, Welling PA (2008) AP-2-dependent internalization of potassium channel Kir2.3 is driven by a novel di-hydrophobic signal. *J Biol Chem* 283:5973–5984.
52. Le Maout S, Brejon M, Olsen O, Merot J, Welling PA (1997) Basolateral membrane targeting of a renal-epithelial inwardly rectifying potassium channel from the cortical collecting duct, CCD-IRK3, in MDCK cells. *Proc Natl Acad Sci USA* 94:13329–13334.
53. Gallolu Kankanamalage S, et al. (2016) Multistep regulation of autophagy by WNK1. *Proc Natl Acad Sci USA* 113:14342–14347.